Reciprocal optical activity in multihelicoidal optical fibers

C. N. Alexeyev,* E. V. Barshak, B. P. Lapin, and M. A. Yavorsky
V. I. Vernadsky Crimean Federal University, Vernadsky Prospekt 4, Simferopol 295007, Crimea, Ukraine

(Received 2 June 2018; published 13 August 2018)

We have studied manifestation of optical activity for higher-order modes that propagate in optical fibers with multihelical distribution of the refractive index profile. We have shown that due to form-induced intermodal coupling between the fundamental modes and the higher-order modes the hybrid modes of such fibers are symmetric (antisymmetric) combinations of circularly polarized optical vortices with opposite orbital angular momentum. We have demonstrated that because of the spin-orbit interaction the system features circular birefringence for such hybrid modes. We have obtained analytical expressions for the coefficients of optical activity related to propagation of such hybrid higher-order modes. We have shown that for those modes the effect of optical activity greatly surpasses the one exhibited for the fundamental modes. The obtained results might be useful for predicting possible new phenomena concerned with propagation of higher-order fields in twisted photonic crystal fibers and for understanding the nature of optical activity for fundamental modes in them.

DOI: 10.1103/PhysRevA.98.023824

I. INTRODUCTION

Optical activity belongs to basic notions of classical optics [1]. Since the discovery of the ability of certain media to rotate the polarization plane of light or, more generally, the axes of its elliptical polarization, this phenomenon is associated with the presence of a circular birefringence. It is manifested in materials with differing refractive indices n_+ and n_- for left and right circularly polarized light, respectively. In such media the polarization plane rotates through an angle γ that turns out to be proportional to the propagation distance z: $\gamma = \pi(n_+ - n_-)z/\lambda$, where λ is the wavelength. Such material optical activity is connected with the presence of chiral molecules in optically active media. Recent progress in fabrication of nanoengineered metamaterials enabled creation of optically active media by introducing structural chirality into a locally nonchiral medium [2–7].

Recent decades have essentially extended our understanding of the mechanisms of inducing optical activity. It has been recognized that this phenomenon may take place in specially engineered optical systems composed of locally nonchiral matter. In such cases the polarization plane can be forced to rotation by bending the path of light. It was shown that this could be achieved by coiling the monomode fiber and thus invoking the topological Berry phase [7–10]. Optical activity is also induced in twisted optical fibers [11,12].

A rather counterintuitive example of that phenomenon has recently been demonstrated in twisted solid-core photonic-crystal fibers (PCFs) [13]. Usually, optical activity in twisted fibers is explained through the presence of two specific directions in the transverse cross-section of the nontwisted fiber with form or material anisotropy, along which polarization vectors of fundamental linearly polarized eigenmodes are directed [14]. Rotation of such axes is assumed to induce the circular birefringence [15]. However, it is impossible to explain the reported optical activity in twisted PCFs [13] due to the presence of such specified directions. Indeed, the PCFs in question possess a multifold symmetry of their cross-sections, so that it is impossible to choose any unique pair of orthogonal axes in the cross-section, along which polarization of eigenmodes should be directed. It is important to note that in Ref. [14] it was implied that such procedure is implementable for any cross-section's form. The wrongness of that (implicit) statement was not understood until publication of Refs. [16,17], where it was pointed out that if the cross-section has a multifold symmetry such a choice of orthogonal directions cannot be made unambiguously. To overcome this difficulty in explaining the experimental results one has to allow for the coupling of the fundamental $\ell = 0$ mode and orbital angular momentum (OAM) modes with higher values of orbital number ℓ, also known as optical vortices (OVs) [18]. Since the wave front of an OV possesses an ℓ-fold symmetry it can be sensitive to the rotation of the cross-section with the same type of symmetry. The physical mechanism responsible for this effect was conventionally called the topological Zeeman effect [19,20]. Later on, with the example of a simplified model of a multihelicoidal fiber (MHF) [21] the importance of the spin-orbit interaction (SOI) in emerging of optical activity in such systems was emphasized [22]. Typical values of $n_+ - n_-$ for such systems proved to be very small—of the order of 10^{-9} RIU (refractive index units)—so that to facilitate observation of that phenomenon it was suggested to study this effect near resonances where fundamental modes are converted in the helical fiber lattice into OVs [23,24]. The existence of such resonance points was previously predicted for chiral fibers [25–30].

In the present paper we resume studying the effects of intermodal coupling in MHFs. All the previous studies were focused on the influence of such coupling on the properties of the fundamental modes. Meanwhile, if the propagation of such modes in MHFs proves to be affected by higher-order modes

*Corresponding author: c.alexeyev@yandex.ua

 ©2018 American Physical Society

there should exist "recoil," reciprocal influence of fundamental modes on the propagation and structure of OAM modes. The aim of this paper is to study the structure and propagation constants of those higher-order modes of MHFs, which are coupled to the fundamental modes through form-induced perturbation, and demonstrate the presence of optical activity for such modes.

II. MODEL AND PERTURBATION THEORY FORMULATION

In a wide sense, a MHF can be determined as a spun optical fiber with a multifold axial symmetry of the refractive index distribution in a cross-section (see Fig. 1 for an example of such a fiber). The lines of constant refractive index value in a MHF form ℓ identical (up to a $2\pi/\ell$ rotation about the fiber's axis) families of helices, which explains the validity of the term "multihelical" for such fibers. Such optical systems are able to change the topological charge of both transmitted and reflected light by either $\pm\ell$ or $\pm(\ell \pm 2)$ (in a.u.) depending on the type of mode coupling that mediates the corresponding transition [27,29,31]. Helical fiber gratings represent a particular case of MHFs [32–35]. At present, MHFs are fabricated by twisting PCFs [23,30].

The refractive index distribution in a MHF can be theoretically modeled in a number of ways [27,28,36]. We prefer to use one of its simplest forms suggested in Ref. [37]:

$$n^2(r,\varphi,z) \approx \tilde{n}^2 - n_{\rm co}^2\Phi(r)\cos\ell(\varphi - qz) = \tilde{n}^2 - \nu^2, \quad (1)$$

where $\tilde{n}^2 = n_{\rm co}^2[1 - 2\Delta f(r)]$; $\nu^2 = n_{\rm co}^2\Phi(r)\cos\ell(\varphi - qz)$; $\Delta \ll 1$ is a dimensionless parameter; f is the profile function that determines the radial dependence of the refractive index in the corresponding "source" ideal fiber, from which the MHF in question is generated; $n_{\rm co}$ is the core's refractive index; $\Phi(r) = 2\Delta\delta r f_r'$, where $f_r' \equiv \frac{df(r)}{dr}$; $\delta \ll 1$ is the dimensionless parameter of the cross-section's deformation; $q = 2\pi/H$; and H is the pitch of the lattice. Here we use cylindrical-polar coordinates (r,φ,z). The electric field in optical fibers satisfies the so-called vector wave equation [38]. If the pitch of the helical lattice is sufficiently large [18], one can neglect the coupling between the transverse electric-field component $\mathbf{E}_t$ and the longitudinal one. In this approximation, the wave equation reduces to

$$(\vec{\nabla}^2 + k^2n^2)\mathbf{E}_t = -\vec{\nabla}_t(\mathbf{E}_t\cdot\vec{\nabla}_t\ln n^2), \quad (2)$$

where k is the wave number in vacuum and $\vec{\nabla}_t = (\partial/\partial x, \partial/\partial y)$.

Since refractive index Eq. (1) depends on z, Eq. (2) is not translational invariant in this variable so that one cannot make the standard substitution, which is widely used in fiber optics: $\mathbf{E}_t = \mathbf{e}_t(r,\varphi)\exp(i\beta z)$, where β is the propagation constant. To restore the translational invariance in Eq. (1) it is necessary to pass to the rotating frame. In effect, this is achieved through passing to new fields $\tilde{e}_\pm = e_\pm\exp(\pm iqz)$, where the fields $e_\pm$ are defined through the components of the transverse vector $\mathbf{e}_t(e_x,e_y)$ as $e_\pm = (e_x \mp ie_y)/\sqrt{2}$. Also one has to introduce new variables $\tilde{r} = r$, $\tilde{z} = z$, and $\tilde{\varphi} = \varphi - qz$. Upon such transformations the wave equation becomes translationally invariant in the $\tilde{z}$ variable, so that one can use the standard substitution: $\tilde{\mathbf{E}}_t(\tilde{r},\tilde{\varphi},\tilde{z}) = \tilde{\mathbf{e}}_t(\tilde{r},\tilde{\varphi})\exp(i\beta\tilde{z})$. This leads to the eigenvalue equation [22]:

$$\left\{\left[\tilde{\nabla}_t^2 + k^2n^2 - (\beta - q\hat{J}_{\tilde{z}})^2 + \hat{H}_{\rm so}\right]\right\}|\tilde{\psi}\rangle = 0, \quad (3)$$

where $|\tilde{\psi}\rangle = {\rm col}(\tilde{e}_+,\tilde{e}_-)$, $\hat{J}_{\tilde{z}} = \hat{l}_{\tilde{z}} + \hat{\tau}_3$, $\hat{l}_{\tilde{z}} = -i\partial/\partial\tilde{\varphi}$, and $\hat{\tau}_i$ is the Pauli matrix. It should be emphasized that in Eq. (3) n^2 is given in terms of the new coordinates $(\tilde{r},\tilde{\varphi},\tilde{z})$ (actually, it is $\tilde{z}$ independent). Here the transverse Laplace operator $\tilde{\nabla}_t^2$ has the standard form in new variables. The operator $\hat{H}_{\rm so}$ arises from the gradient term in Eq. (1) and, essentially, describes the SOI. Its explicit form is [22]

$$\hat{H}_{\rm so} = (2\psi + \tilde{r}\psi'_{\tilde{r}} + \tilde{r}\psi\nabla_{\tilde{r}})\hat{\tau}_0 + \psi\hat{\tau}_3\hat{l}_{\tilde{z}} + \begin{pmatrix} 0 & \exp(-2i\tilde{\varphi})\hat{a}_+ \\ \exp(2i\tilde{\varphi})\hat{a}_- & 0 \end{pmatrix}, \quad (4)$$

where $\hat{a}_\pm = \tilde{r}\psi\nabla_{\tilde{r}} + \tilde{r}\psi'_{\tilde{r}} \pm \psi\hat{l}_{\tilde{z}}$ and $\psi = \Delta f'_{\tilde{r}}/\tilde{r}$.

The main idea of Ref. [22] on obtaining the analytical expressions for optical activity was to study the effect of twisting (chirality) on the propagation constants of circularly polarized fundamental modes on the background of intermodal coupling and SOI. In that paper it was found that combination of chirality and intermodal coupling results in the dependence of the propagation constant value on the polarization sign. To take advantage of the same approach one has first to make necessary changes to the perturbation theory used in Ref. [22]. Such changes concern the choice of the zero-approximation state, to which the corrections are found. Following the cited paper, we start from the notion that the propagation of light in ideal fibers is governed in the scalar approximation by the Hamiltonian $\hat{H}_0 = \tilde{\nabla}_t^2 + k^2\tilde{n}^2$ [18,38]. The eigenvalue equation $\hat{H}_0|\psi_0\rangle = \tilde{\beta}^2|\psi_0\rangle$ yields the eigenvectors $|\psi_0\rangle$, which describe the fiber modes in the scalar approximation, and scalar propagation constants $\tilde{\beta}$. The eigenvectors $|\psi_0\rangle$ can be chosen in the form of OVs $|\sigma,m\rangle$ [18]. In the basis of linear polarizations $|e\rangle = {\rm col}(e_x,e_y)$ their expressions read as

$$|\sigma,m\rangle = \begin{pmatrix} 1 \\ i\sigma \end{pmatrix}\exp(im\tilde{\varphi})F_m(\tilde{r}), \quad (5)$$

where $\sigma = \pm 1$ determines the sign of circular polarization, the orbital number m specifies the topological charge of this

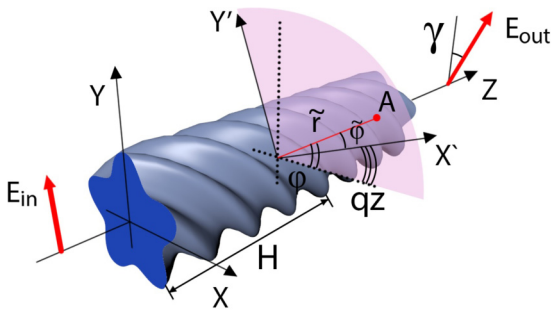

FIG. 1. The model of a MHF ($\ell = 5$) and the geometry of the problem. In a cross-section z the frame $X'Y'$ rotated by an angle qz with respect to laboratory frame XY is introduced, in which a point A has polar coordinates $\tilde{r} = r, \tilde{\varphi} = \varphi - qz$ (also $\tilde{z} = z$). There are shown the pitch H and rotation of the electric vector $\mathbf{E}_{\rm out}$ of the outcoming field by an angle γ with respect to the vector $\mathbf{E}_{\rm in}$ of the incoming field.

vortex solution, and the radial function F_m satisfies the known equation [38].

It is well established that the spectrum $\tilde{\beta}_m$ is fourfold degenerate for $m > 1$ and twofold degenerate at $m = 0$. This circumstance introduces the difference between the actions exerted on ideal-fiber mode structure by the intermodal coupling in form-perturbed fibers. Indeed, if for a circularly polarized fundamental mode such weak coupling can only shift the value of its propagation constant, for higher-order modes this may result in the changing of the very mode structure. Indeed, there are two OVs of the same polarization ($|\sigma, m\rangle$ and $|\sigma, -m\rangle$) that belong to the eigenvalue $\tilde{\beta}_m$. Here we allow for the fact that perturbation of the form does not couple the states with different polarizations. In this way, prior to studying the combined effects of SOI and chirality, one has to determine the modes of the fiber with refractive index distribution given by Eq. (1) at $q = 0$.

To this end, it is convenient to apply perturbation theory with degeneracy to the equation $(\tilde{\nabla}_t^2 + k^2 n^2)|\bar{\psi}\rangle = \bar{\beta}^2|\bar{\psi}\rangle$ treating the term $-\nu^2$ as perturbation [39]. Here $|\bar{\psi}\rangle$ is the eigenfunction of the Hamiltonian $\tilde{\nabla}_t^2 + k^2 n^2$, that is, the one which describes the nonhelical (nontwisted) straight fiber with the refractive index modulated by the perturbation $-n_{\text{co}}^2 \Phi(r)\cos\ell(\varphi - qz)$ (which renders the core a characteristic multipetal form), and $\bar{\beta}^2$ is the corresponding eigenvalue. To establish the structure of modes that appears due to intermodal coupling one has to build the matrix H_0 of the operator $\tilde{\nabla}_t^2 + k^2 n^2 - \bar{\beta}^2$ over the basis of those eigenvectors of $\hat{H}_0$, which can be coupled by such operator. Since $\hat{H}_0$ couples only the states with $m = 0$, $m = \pm\ell$, and the same polarization, one should search for the eigenvectors in the following orthogonal subspaces:

$$|1, 0\rangle,\ |1, \ell\rangle, |1, -\ell\rangle \tag{6}$$

and

$$|-1, 0\rangle,\ |-1, \ell\rangle, |-1, -\ell\rangle. \tag{7}$$

The eigenvector equation $H_0\vec{x} = \bar{\beta}^2\vec{x}$ in the first subspace Eq. (6) leads to the following eigenvalue problem:

$$\begin{vmatrix} \tilde{\beta}_0^2 - \bar{\beta}^2 & Q & Q \\ Q & \tilde{\beta}_\ell^2 - \bar{\beta}^2 & 0 \\ Q & 0 & \tilde{\beta}_\ell^2 - \bar{\beta}^2 \end{vmatrix} = 0, \tag{8}$$

where $Q = \langle\sigma, 0| - k^2\nu^2|\sigma, \ell\rangle$ is the coupling constant and the scalar product is defined as $\langle\Phi \mid \Psi\rangle = \iint_S (\Phi_+^* \Phi_-^*)\binom{\Psi_+}{\Psi_-} dS$, where S is the total transverse cross-section of the fiber. For step-index fibers $Q = -k^2 n_{\text{co}}^2 \delta\Delta/\sqrt{N_0 N_\ell}$, where the normalization coefficient is $N_m = \int_0^\infty x F_m^2 dx$. In the limiting case of small form perturbation on the background of a large splitting of scalar propagation constants, $|Q| \ll |\tilde{\beta}_\ell^2 - \tilde{\beta}_0^2|$, one has for the spectrum of $\bar{\beta}^2$

$$\bar{\beta}_1^2 = \tilde{\beta}_\ell^2, \quad \bar{\beta}_2^2 = \tilde{\beta}_0^2 + Q^2/\varsigma\tilde{\beta}_0, \quad \bar{\beta}_3^2 = \tilde{\beta}_\ell^2 - Q^2/\varsigma\tilde{\beta}_0, \tag{9}$$

where $\varsigma = \tilde{\beta}_0 - \tilde{\beta}_\ell$ and we allowed for the fact that $\varsigma \ll \tilde{\beta}_0$. The expressions for the corresponding modes in the limit $\varsigma \ll \tilde{\beta}_0$ look like

$$\begin{aligned} \psi_1 &\propto |1, \ell\rangle - |1, -\ell\rangle, \\ \psi_2 &\propto |1, 0\rangle + \frac{Q}{2\tilde{\beta}_0\varsigma}(|1, \ell\rangle + |1, -\ell\rangle), \\ \psi_3 &\propto \frac{-Q}{\tilde{\beta}_0\varsigma}|1, 0\rangle + |1, \ell\rangle + |1, -\ell\rangle. \end{aligned} \tag{10}$$

In the second subspace Eq. (7) the eigenvalue problem Eq. (8) has the same form, so that the spectrum Eq. (9) does not change:

$$\bar{\beta}_1^2 = \bar{\beta}_4^2, \quad \bar{\beta}_2^2 = \bar{\beta}_5^2, \quad \bar{\beta}_3^2 = \bar{\beta}_6^2, \tag{11}$$

and the modes are

$$\begin{aligned} \psi_4 &\propto |-1, \ell\rangle - |-1, -\ell\rangle, \\ \psi_5 &\propto |-1, 0\rangle + \frac{Q}{2\tilde{\beta}_0\varsigma}(|-1, \ell\rangle + |-1, -\ell\rangle), \\ \psi_6 &\propto \frac{-Q}{\tilde{\beta}_0\varsigma}|-1, 0\rangle + |-1, \ell\rangle + |-1, -\ell\rangle. \end{aligned} \tag{12}$$

As is evident, the intermodal coupling in such form-perturbed fibers changes the mode structure of higher-order modes. The hybridized modes are combinations of circularly polarized higher-order ideal fiber modes $|\sigma, \ell\rangle \pm |\sigma, -\ell\rangle$ and fundamental modes $|\sigma, 0\rangle$. However, it is not necessary to retain in such expressions relatively small terms proportional to $Q/\tilde{\beta}_0\varsigma \ll 1$. The main effect of form perturbation turns out to be the lifting of degeneracy for $|1, \pm\ell\rangle$ modes with simultaneous merging of them into Hermite-Gaussian-like fields. Now we are in a position to calculate the corrections to propagation constants of these scalar-approximation modes, which are induced by the combined action of the twisting and the SOI.

III. RECIPROCAL OPTICAL ACTIVITY

As in the case of optical activity for fundamental modes, the SOI-induced renormalization of propagation constants does not lead to their splitting in polarization. Indeed, the eigenvalue equation for the case of subspace Eq. (6) has the form

$$\begin{vmatrix} \tilde{\beta}_0^2 - \beta^2 & Q & Q \\ Q & \tilde{\beta}_\ell^2 + \alpha\ell - \beta^2 & 0 \\ Q & 0 & \tilde{\beta}_\ell^2 - \alpha\ell - \beta^2 \end{vmatrix} = 0, \tag{13}$$

where the SOI constant $\alpha = \Delta/r_0^2 N_\ell$ and r_0 is the core's radius. For the case of subspace Eq. (7) the corresponding equation can be obtained from Eq. (13) by inverting the sign of α. Since the eigenvalue equation Eq. (13) is symmetric in α,

$$\left[\tilde{\beta}_0^2 - \beta^2\right]\left\{\left[\tilde{\beta}_\ell^2 - \beta^2\right]^2 - \ell^2\alpha^2\right\} - 2Q^2\left(\beta_\ell^2 - \beta^2\right) = 0, \tag{14}$$

then the SOI-induced corrections to spectra are insensitive to the sign of α and the polarization of basic fields. Left and right circularly polarized fields in this case propagate with the same phase velocity and no circular birefringence appears in the system.

To allow for twisting it is necessary to average the operator on the left of Eq. (3) over the basis Eqs. (6) and (7). The

resulting eigenvalue equation for the subspace Eq. (6) takes on the form

$$\begin{vmatrix} \tilde{\beta}_0^2 - (\beta - q)^2 & Q & Q \\ Q & \tilde{\beta}_\ell^2 + \alpha\ell - (\beta - q - q\ell)^2 & 0 \\ Q & 0 & \tilde{\beta}_\ell^2 - \alpha\ell - (\beta - q + q\ell)^2 \end{vmatrix} = 0. \tag{15}$$

For the subspace Eq. (7) the analogous equation reads as

$$\begin{vmatrix} \tilde{\beta}_0^2 - (\beta + q)^2 & Q & Q \\ Q & \tilde{\beta}_\ell^2 - \alpha\ell - (\beta + q - q\ell)^2 & 0 \\ Q & 0 & \tilde{\beta}_\ell^2 + \alpha\ell - (\beta + q + q\ell)^2 \end{vmatrix} = 0. \tag{16}$$

We will assume that the twist rate and the influence of the SOI are small, so that the eigenmodes are still given by Eqs. (10) and (12). Then it is sufficient to obtain the corrections to eigenvalues.

Due to the effect of the rotating frame the corrections to zero-approximation eigenvalues do not vanish even in the absence of intermodal coupling and the SOI. To separate such corrections, which should vanish upon transition to the laboratory frame, it is helpful to notice that if one first sets $\beta \equiv \bar{\beta} + q$ in Eq. (15) then one arrives at Eq. (8) in the subsequent limit $\alpha, q \to 0$. From this fact one can infer the rule for representing the corrections to propagation constants $\bar{\beta}_i^2$ for modes Eqs. (10) and (12). According to it, the propagation constants of modes $\psi_{1,4}$ should be sought for as

$$\beta_{1,4} = \bar{\beta}_{1,4} \pm q + \varepsilon_\pm, \tag{17}$$

where $\varepsilon_\pm$ is the desired correction and the upper sign corresponds to the first listed mode. Analogously,

$$\beta_{3,6} = \bar{\beta}_{4,6} \pm q + \varepsilon'_\pm. \tag{18}$$

Note that here we are not interested in corrections to propagation constants of the fundamental modes. After a little algebra, one can obtain

$$\varepsilon_\pm = -\varepsilon'_\pm = \frac{\varsigma\ell^2}{2Q^2}(2q\tilde{\beta}_0 \pm \alpha)^2. \tag{19}$$

To show the presence of optical activity for higher-order modes it is helpful to get the expressions for modes $\psi_{1,4}$ and $\psi_{3,6}$ in the laboratory frame:

$$\psi_{1,4} \propto \sin[\ell(\varphi - qz)]\begin{pmatrix} 1 \\ \pm i \end{pmatrix} \exp[i(\tilde{\beta}_\ell + \varepsilon_\pm)z],$$
$$\psi_{3,6} \propto \cos[\ell(\varphi - qz)]\begin{pmatrix} 1 \\ \pm i \end{pmatrix} \exp\left[iz\left(\tilde{\beta}_\ell - \frac{Q^2}{2\varsigma\tilde{\beta}_0} - \varepsilon_\pm\right)\right], \tag{20}$$

where we have omitted insignificant radial factors. If one creates at the input end of such a fiber an x-polarized field with azimuthal dependence of, say, $\sin\ell\varphi$, then within the fiber it would evolve (in the basis of linear polarizations) as $\propto \sin[\ell(\varphi - qz)]\mathrm{col}(\cos\delta\beta z, -\sin\delta\beta z)$, where $\delta\beta = (\beta_1 - \beta_4 - 2q)/2$. Note that here the term $-2q$ appears due to the transition to the laboratory frame. The first feature of such evolution is the rotation of intensity distribution at a rate q, which was previously demonstrated for elliptical twisted fibers [40]. The second, and more important to us, is the polarization plane rotation, which corresponds to the optical activity A of the value:

$$A \equiv \frac{\pi(n_+ - n_-)}{\lambda} = \frac{(\beta_1 - q) - (\beta_4 + q)}{2} \approx 2\alpha q\tilde{\beta}_0\varsigma\ell^2 Q^{-2}. \tag{21}$$

As is evident from Eq. (20), an analogous input field with the azimuthal dependence of $\cos\ell\varphi$ should feature the optical activity of the $-A$ value. In this way, optical activity for higher-order modes turns out to be dependent on their oddity. This property of optical activity's sign to depend on the oddity of the state has been hitherto unknown and is a unique feature of MHFs.

It is helpful to compare the values of optical activity for higher-order modes and the fundamental modes. For the latter case one can obtain in the same manner

$$A_{\mathrm{FM}} = \frac{Q^2\ell^2\alpha q}{2\varsigma^3\tilde{\beta}_0^3}, \tag{22}$$

which correlates with the corresponding result of Ref. [22]. The comparison of the values of optical activities yields through Eqs. (21) and (22) for their ratio

$$\frac{A}{A_{\mathrm{FM}}} \propto \left(\frac{\varsigma\tilde{\beta}_0}{Q}\right)^4. \tag{23}$$

Since $|Q| \ll |\tilde{\beta}_\ell^2 - \tilde{\beta}_0^2|$ it follows that $A \gg A_{\mathrm{FM}}$, so that the magnitude of optical activity for higher-order modes is much greater than the one for the fundamental modes. Some data on the magnitudes of optical activities and their dependence on fiber parameters are presented in Figs. 2 and 3. Figure 4 shows also the dependence of $n_+ - n_-$ and A/A_{FM} on wavelength.

It is also worth emphasizing the differences between the approaches of the present paper and Ref. [22] used for solving the problem of optical activity. Both approaches are based on finding SOI and twist-induced corrections to zero-approximation roots of corresponding eigenvalue equations. In Ref. [22] we concentrated on finding such corrections to eigenvalues $\tilde{\beta}_0^2$ of ideal fiber fundamental modes. From a formal point of view, in the present paper we also could have chosen the analogous scenario of obtaining corrections to eigenvalues $\tilde{\beta}_\ell^2$ of degenerate OVs. The drawback of such a head-on approach is that such corrections can be easily misinterpreted as correction to propagation constants of OVs, whereas the corresponding eigenmodes may differ from pure OVs. Actually, this is just

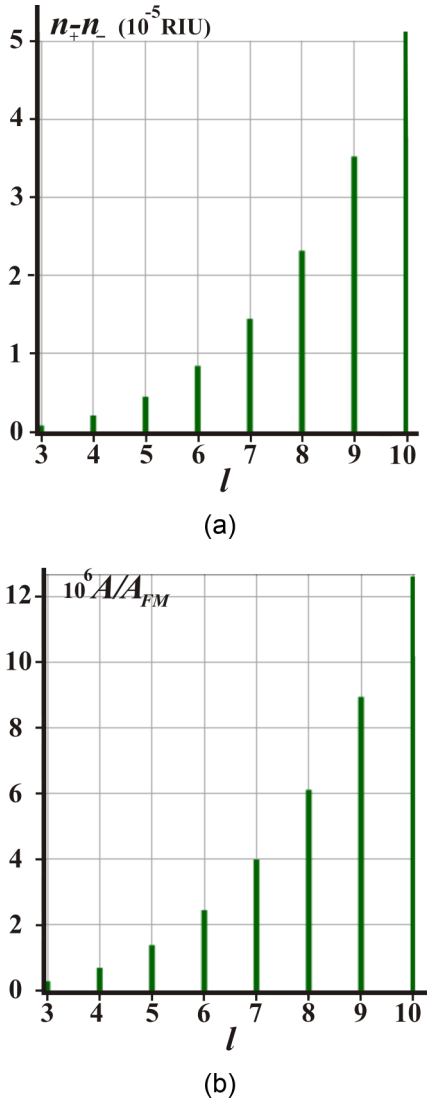

FIG. 2. The difference $n_+ - n_-$ in refractive index units (RIU) for higher-order modes at various orders of fiber symmetry ℓ (a) and the ratio of optical activities $A/A_{\rm FM}$ of higher-order modes and the fundamental mode (b). Fiber parameters: $n_{\rm co} = 1.5$, $r_0 = 20\lambda_0$, $\lambda_0 = 800$nm, $\delta = 0.05$, $q = 5\text{m}^{-1}$, $\Delta = 0.05$.

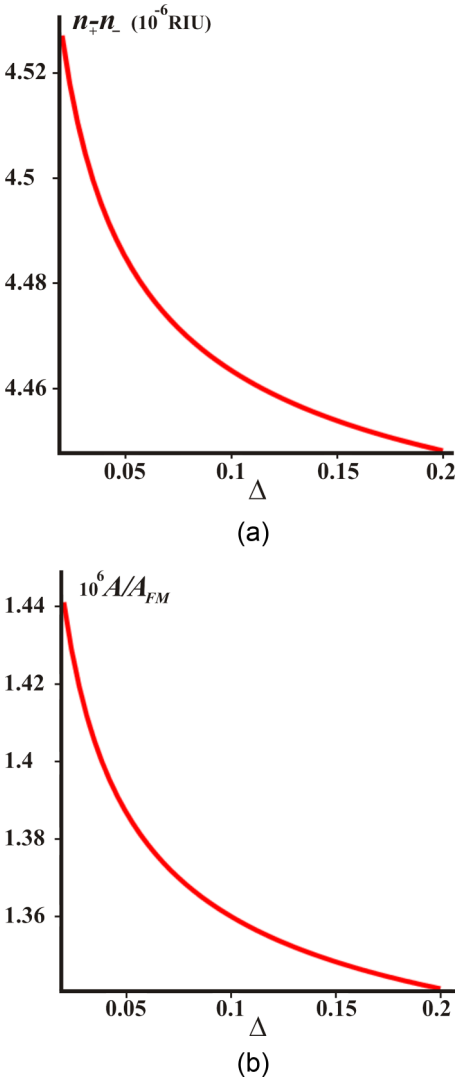

FIG. 3. The difference $n_+ - n_-$ (in RIU) vs the height of refractive index profile Δ (a) and the ratio of optical activities $A/A_{\rm FM}$ vs Δ for higher-order modes and the fundamental mode (b); $\ell = 5$, other parameters as in Fig. 2.

the case: due to degeneracy perturbation changes the structure of the ground state and the obtained corrections correspond to propagation constants of $|1, \ell\rangle \pm |1, -\ell\rangle$ combinations of OVs [see, for example, Eq. (10)]. We believe that by a proper treatment of eigenvalue problems Eqs. (15) and (16) one can get the correct results on mode structure. However, in the present paper we have chosen a somewhat different approach based on consecutively accounting for the perturbation factors. First, we obtained the mode structure and propagation constants in the absence of SOI and twisting [see Eqs. (9)–(12)]. Second, we obtained corrections to propagation constants of such hybrid modes induced by SOI and twisting. In such step by step approach we are able to control physical meaning of results and minimize misinterpretation mistakes.

To understand the nature of the obtained difference in magnitudes of optical activity for higher-order and fundamental modes it is helpful to note that, mathematically, it stems from different renormalization of roots Eq. (9) [which can be also obtained from Eq. (15) at $\alpha = 0$, $q = 0$] by switching on the SOI ($\alpha \neq 0$) and the twisting ($q \neq 0$). Schematically, such renormalizations can be illustrated by the following simple example. Assume first that some third-order polynomial has two closely spaced roots $x_{1,2}$, whereas the third root x_3 obeys $|x_1 - x_2| \ll |x_3 - x_{1,2}|$. Let this polynomial be perturbed with a constant $\kappa \ll 1$. Then the renormalized roots $\tilde{x}_i$ are found from the equation

$$(x - x_1)(x - x_2)(x - x_3) + \kappa = 0. \tag{24}$$

To obtain renormalization of neighboring $x_{1,2}$ roots it is sufficient to set in their vicinity $x - x_3 \approx x_{1,2} - x_3 \equiv \xi$ in Eq. (24). Then at $|\kappa/\xi| \ll (x_1 - x_2)^2$ the renormalized roots $\tilde{x}_{1,2}$ read as

$$\tilde{x}_{1,2} \approx x_{1,2} \mp \frac{\kappa}{\xi(x_1 - x_2)}. \tag{25}$$

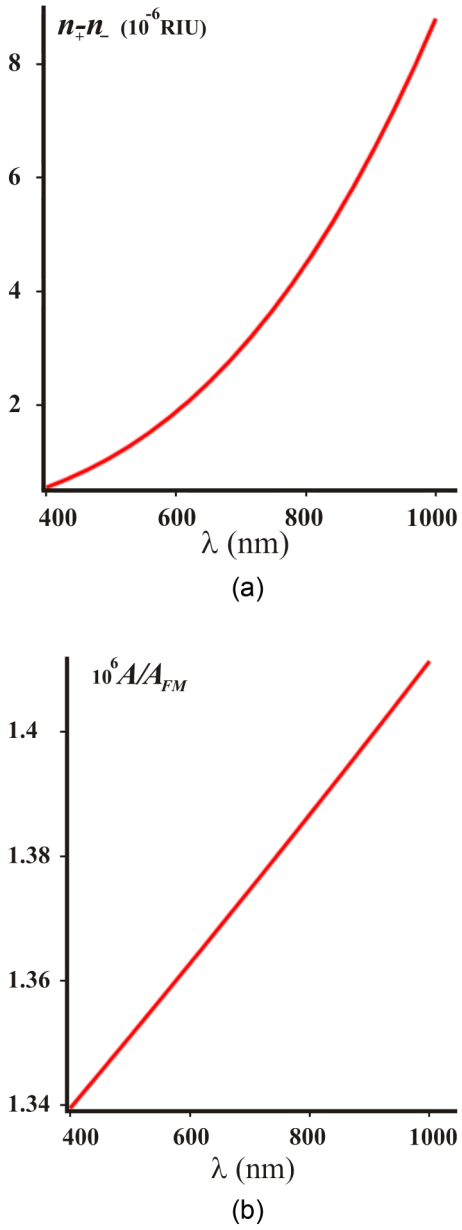

FIG. 4. The difference $n_+ - n_-$ (in RIU) vs wavelength (a) and the ratio of optical activities $A/A_{\rm FM}$ vs wavelength (b); $\ell = 5$, other parameters as in Fig. 2.

The situation is quite different for the remaining "separated" root x_3: near this root Eq. (24) is transformed into $\xi^2(x - x_3) + \kappa = 0$, which gives

$$\tilde{x}_3 = x_3 - \kappa\xi^{-2}. \tag{26}$$

For the shifts of these roots $\Delta x_i = x_i - \tilde{x}_i$ one can obtain the following result:

$$\left|\frac{\Delta x_{1,2}}{\Delta x_3}\right| = \left|\frac{x_{1,2} - x_3}{x_1 - x_2}\right|. \tag{27}$$

Since $|x_1 - x_2| \ll |x_{1,2} - x_3|$ one arrives at

$$|\Delta x_{1,2}| \gg |\Delta x_3|, \tag{28}$$

that is, perturbation-induced renormalization of closely spaced levels is much greater than the one of solitary ones. In our case the roots $\bar{\beta}_1^2$ and $\bar{\beta}_3^2$ in Eq. (9) play the role of $x_{1,2}$ roots, whereas $\bar{\beta}_2^2$ corresponds to the x_3 root. Using here the values of spectra Eq. (9) gives for the ratio in Eq. (27), $(\varsigma\tilde{\beta}_0/Q)^2$, which qualitatively correlates with the result Eq. (23), although it gives a wrong power. This discrepancy can be explained through a much more complicated form of the perturbing term implied by Eq. (15), as well as through the differences in corresponding polynomials. Naturally, this algebra is rooted in the fact of double degeneracy of propagation constants for higher-order modes of ideal fibers. Although form perturbation $k^2\nu^2$ lifts it, still, the corresponding levels $\bar{\beta}_{1,3}^2$ remain closely spaced. It should be stressed, however, that despite the fact that the shift of closely spaced levels (roots) $x_{1,2}$ given by Eq. (25) can be understood also as the well-known phenomenon of repulsion of energy levels, the final result Eq. (27) on the ratio of energy-level shifts is, to the best of our knowledge, hitherto unreported in the literature.

It is widely recognized that the phenomenon of optical activity in twisted PCFs and MHFs is the effect of the SOI. However, in explanations of SOI-related phenomena it is usually implied that spinning photons possess their own intrinsic OAM. Our example demonstrates that this requirement is not necessary for manifestation of the SOI-related phenomena. Indeed, from the presented theory it follows that at the first stage the intermodal coupling induced by the form perturbation generates the mode structure given by Eqs. (10) and (12). Its main feature is the merging of partial OVs $|\sigma, \pm\ell\rangle$ with well-defined OAM into combinations $|\sigma, \ell\rangle \pm |\sigma, -\ell\rangle$ with no OAM. Since the intensity of the field in such combinations is modulated by $\cos\ell\varphi$ and $\sin\ell\varphi$ factors, they became sensitive to twisting of the refractive index profile modulated by the $\cos\ell\varphi$ factor. The photons in such superpositions are forced then to follow the spiral trajectories. It is well established by now that a spinning photon moving along a spiral path in a guiding medium experiences in the acts of total internal reflections the transverse shifts with respect to its momentum vector [41]. The combined effect of such shifts depends on the sign of the photon's spin and, in this way, constitutes the influence of the spin on the photon's trajectory. Being a manifestation of the SOI, such optical Magnus effect can be also regarded as a consequence of the Imbert-Fedorov effect [42]. It should be emphasized that in guiding media OAM-carrying photons propagate along curved trajectories as dictated by Poynting vector lines for such objects. In our case the situation is quite different: whereas the combinations $|\sigma, \ell\rangle \pm |\sigma, -\ell\rangle$ bear neither OAM nor φ-dependent phase multipliers, which could have inclined their Poynting vectors to the transverse plane and made the trajectory spiral, the photons are forced to move along such spiraling trajectories by the geometry of a twisting refractive index profile. However, once they are made to spiral, they are influenced by the same factors as OAM-carrying photons in ideal fibers and exhibit an analogous dependence of trajectories on the spin value, which is conventionally attributed to the SOI.

Regretfully, based on this interpretation we can provide only qualitative physical explanation of the fact that optical activity for higher-order modes much surpasses the one for the fundamental modes as expressed by Eq. (23). Let us assume

that the magnitude of the effect is proportional to the fraction of the profile-sensitive combinations $|\sigma, \ell\rangle \pm |\sigma, -\ell\rangle$ in the structure of hybrid modes Eqs. (10) and (12). Then if one takes the magnitude of optical activity for modes $\psi_{1,3}$ (or $\psi_{4,6}$), which are approximately given by such profile-sensitive fields $|\sigma, \ell\rangle \pm |\sigma, -\ell\rangle$, for unity, this effect for the modes $\psi_{2,5}$ should be of lesser magnitude. Indeed, in those modes the fraction of $|\sigma, \ell\rangle \pm |\sigma, -\ell\rangle$ fields is of order $Q/\tilde{\beta}_0\varsigma \ll 1$, which gives for powers stored in such combinations of OVs an even stronger estimate of $(Q/\tilde{\beta}_0\varsigma)^2$. Although we do not obtain here an exact coincidence with Eq. (23) that implies quadratic dependence on relative power, this indicates the relevance of profile-sensitive fields in the structure of hybrid modes.

The last comment concerns the role of intermodal coupling in forming optical activity for fundamental and higher-order modes. Being twisting insensitive fundamental modes need to be coupled to higher-order modes, which react on the fiber twisting. This is expressed through proportionality of optical activity A_{FM} to the coupling parameter Q in Eq. (22): at $Q = 0$ the effect vanishes. The situation is seemingly different for optical activity for higher-order modes Eq. (21), which at $Q \to 0$ does not vanish. Indeed, the combinations $|\sigma, \ell\rangle \pm |\sigma, -\ell\rangle$ are twisting sensitive even in the absence of the small fraction of fundamental modes and in this way seem to not require any intermodal coupling. Although this is true, one should bear in mind that the very origin of such combinations of OVs is based on the intermodal coupling: if one sets $Q = 0$ in Eq. (8) one does not arrive at the hybrid mode structure given by Eqs. (10) and (12). In addition, the result given by Eq. (21) is valid only for intermodal exchange greater than the spin-orbit coupling and does not permit the limiting transition $Q \to 0$. The obtained results might be useful both for understanding the nature of optical activity for fundamental modes in twisted PCFs and for predicting possible new phenomena in them, which relate to propagation of higher-order fields.

IV. CONCLUSION

In the present paper we have studied manifestation of optical activity for higher-order modes that propagate in optical fibers with multihelical distribution of the refractive index profile. We have shown that a specific perturbation of the ideal fiber form that exists in such multihelicoidal fibers leads to forming the mode structure, in which circularly polarized fundamental $\ell = 0$ modes are hybridized with circularly polarized symmetric and antisymmetric combinations of optical vortices with opposite OAM numbers and equal moduli ℓ. Such zero-OAM combinations due to azimuthal-inhomogeneous energy distribution in them prove to be sensitive to the spiraling of the refractive index profile that makes them adiabatically follow the refractive index pattern. Because of the spin-orbit interaction, the propagation constants for such hybridized modes turn out to depend on their spin sign, which leads to the circular birefringence for higher-order modes and the resulting enhanced optical activity for them. We have demonstrated that optical activity for higher-order modes in such a system greatly exceeds the one for the fundamental modes previously reported in the literature.

ACKNOWLEDGMENTS

The authors acknowledge Russian Foundation for Basic Research Grant No. 17-42-92014 and V. I. Vernadsky Crimean Federal University Grant No. ВГ01/2017.

[1] E. Hecht, *Optics*, 2nd ed. (Addison-Wesley, Reading, MA, 1987).

[2] A. Lakhtakia and R. Messier, *Sculptured Thin Films: Nanoengineered Morphology and Optics* (SPIE, Bellingham, WA, 2005).

[3] Y. Saito and H. Hyuga, Homochirality: Symmetry breaking in systems driven far from equilibrium, Rev. Mod. Phys. **85**, 603 (2013).

[4] Z. Li, M. Mutlu, and E. Ozbay, Chiral metamaterials: From optical activity and negative refractive index to asymmetric transmission, J. Opt. **15**, 023001 (2013).

[5] G. M. Grason, Geometry and optimal packing of twisted columns and filaments, Rev. Mod. Phys. **87**, 401 (2015).

[6] S. Behera and J. Joseph, N-single-helix photonic-metamaterial based broadband optical range circular polarizer by induced phase lags between helices, Appl. Opt. **54**, 1212 (2015).

[7] T. Verbiest, G. Koeckelberghs, and B. Champagne, Feature issue introduction: Chirality in optics, Opt. Mater. Express **4**, 2663 (2014).

[8] R. Y. Chiao and Y.-S. Wu, Manifestation of Berry's Topological Phase for the Photon, Phys. Rev. Lett. **57**, 933 (1986).

[9] A. Tomita and R. Y. Chiao, Observation of Berry's Topological Phase by use of an Optical Fibre, Phys. Rev. Lett. **57**, 937 (1986).

[10] M. V. Berry, Interpreting the anholonomy of coiled light, Nature (London) **326**, 277 (1987).

[11] R. Ulrich and A. Simon, Polarization optics of twisted single-mode fibres, Appl. Opt. **18**, 2241 (1979).

[12] E. V. Barshak, C. N. Alexeyev, B. P. Lapin, and M. A. Yavorsky, Twisted anisotropic fibers for robust orbital-angular-momentum-based information transmission, Phys. Rev. A **91**, 033833 (2015).

[13] X. M. Xi, T. Weiss, G. K. L. Wong, F. Biancalana, S. M. Barnett, M. J. Padgett, and P. St. J. Russell, Optical Activity in Twisted Solid-Core Photonic Crystal Fibers, Phys. Rev. Lett. **110**, 143903 (2013) ; P. S. J. Russell, R. Beravat, and G. K. L. Wong, Helically twisted photonic crystal fibres, Phil. Trans. R. Soc. A **375**, 20150440 (2017) ; M. Napiorkowski and W. Urbanczyk, Scaling effects in resonant coupling phenomena between fundamental and cladding modes in twisted microstructured optical fibers, Opt. Express **26**, 12131 (2018); Role of symmetry in mode coupling in twisted microstructured optical fibers, Opt. Lett. **43**, 395 (2018).

[14] A. W. Snyder and X. H. Zheng, Optical fibers of arbitrary crosssections, J. Opt. Soc. Am. A **3**, 600 (1986).

[15] A. J. Barlow, J. J. Ramskovhansen, and D. N. Payne, Birefringence and polarization mode-dispersion in spun single-mode fibers, Appl. Opt. **20**, 2962 (1981).

[16] M. Steel, T. P. White, C. M. de Sterke, R. C. McPhedran, and L. C. Botten, Symmetry and degeneracy in microstructured optical fibers, Opt. Lett. **26**, 488 (2001).

[17] K. Z. Aghaie, V. Dangui, M. J. F. Digonnet, S. Fan, and G. S. Kino, Classification of the core modes of hollow-core photonicbandgap fibers, IEEE J. Quantum Electron. **45**, 1192 (2009).

[18] C. N. Alexeyev, A. V. Volyar, and M. A. Yavorsky, Fiber optical vortices, in *Lasers, Optics and Electro-Optics Research Trends*, edited by L. I. Chen (Nova, New York, 2007), pp. 131–223.

[19] T. Weiss, G. K. L. Wong, F. Biancalana, S. M. Barnett, X. M. Xi, and P. St. J. Russell, Topological Zeeman effect and circular birefringence in twisted photonic crystal fibers, J. Opt. Soc. Am. B **30**, 2921 (2013).

[20] L. Chen, W.-G. Zhang, T.-Y. Yan, L. Wang, J. Sieg, B. Wang, Q. Zhou, and L.-Y. Zhang, Photonic crystal fiber polarization rotator based on the topological Zeeman effect, Opt. Lett. **40**, 3448 (2015).

[21] C. N. Alexeyev, Generation of optical vortices in spun multihelicoidal optical fibers, Appl. Opt. **51**, 6125 (2012).

[22] C. N. Alexeyev, B. P. Lapin, G. Milione, and M. A. Yavorsky, Optical activity in multihelicoidal optical fibers, Phys. Rev. A **92**, 033809 (2015).

[23] G. K. L. Wong, X. M. Xi, M. H. Frosz, and P. St. J. Russell, Enhanced optical activity and circular dichroism in twisted photonic crystal fiber, Opt. Lett. **40**, 4639 (2015).

[24] C. N. Alexeyev, B. P. Lapin, and M. A. Yavorsky, Resonance optical activity in multihelicoidal optical fibers, Opt. Lett. **41**, 962 (2016).

[25] C. N. Alexeyev and M. A. Yavorsky, Generation and conversion of optical vortices in long-period helical core optical fibers, Phys. Rev. A **78**, 043828 (2008).

[26] C. N. Alexeyev, T. A. Fadeyeva, B. P. Lapin, and M. A. Yavorsky, Generation of optical vortices in layered helical waveguides, Phys. Rev. A **83**, 063820 (2011).

[27] H. Xu and L. Yang, Conversion of orbital angular momentum of light in chiral fiber gratings, Opt. Lett. **38**, 1978 (2013).

[28] Y. V. Kartashov, V. A. Vysloukh, and L. Torner, Dynamics of topological light states in spiraling structures, Opt. Lett. **38**, 3414 (2013).

[29] C. N. Alexeyev, A. N. Alexeyev, B. P. Lapin, G. Milione, and M. A. Yavorsky, Spin-orbit-interaction-induced generation of optical vortices in multihelicoidal fibers, Phys. Rev. A **88**, 063814, (2013).

[30] G. K. Wong, M. S. Kang, H. W. Lee, F. Biancalana, C. Conti, T. Weiss, and P. St. J. Russell, Excitation of orbital angular momentum resonances in helically twisted photonic crystal fiber, Science **337**, 446 (2012).

[31] C. N. Alexeyev, Narrowband reflective generation of higher-order optical vortices in Bragg spun optical fibers, Appl. Opt. **52**, 433 (2013).

[32] R. D. Birch, Fabrication and characterisation of circularly birefringent helical fibres, Electron. Lett. **23**, 50 (1987).

[33] C. D. Poole, C. D. Townsend, and K. T. Nelson, Helical-grating two-mode fiber spatial-mode coupler, J. Lightwave Technol. **9**, 598 (1991).

[34] V. I. Kopp, V. M. Churikov, J. Singer, N. Chao, D. Neugroschl, and A. Z. Genack, Chiral fiber gratings, Science **305**, 74 (2004).

[35] V. I. Kopp and A. Z. Genack, Adding twist, Nat. Photonics **5**, 470 (2011).

[36] X. M. Xi, G. K. L. Wong, M. H. Frosz, F. Babic, G. Ahmed, X. Jiang, T. G. Euser, and P. St. J. Russell, Orbital-angular-momentum-preserving helical Bloch modes in twisted photonic crystal fiber, Optica **1**, 165 (2014).

[37] C. N. Alexeyev, A. V. Volyar, and M. A. Yavorsky, Multi-helix chiral fibre filters of higher-order optical vortices, J. Opt. A **9**, 537 (2007).

[38] A. W. Snyder and J. D. Love, *Optical Waveguide Theory* (Chapman and Hall, London, 1985).

[39] A. S. Davydov, *Quantum Mechanics* (Pergamon, Oxford, 1976).

[40] C. N. Alexeyev and M. A. Yavorsky, Optical vortices and the higher order modes of twisted strongly elliptical optical fibres, J. Opt. A **6**, 824 (2004).

[41] V. S. Liberman and B. Ya. Zel'dovich, Spin-orbit interaction of a photon in an inhomogeneous medium, Phys. Rev. A. **46**, 5199 (1992).

[42] K. Y. Bliokh, A. Niv, V. Kleiner, and E. Hasman, Geometrodynamics of spinning light, Nat. Photonics **2**, 748 (2008); K. Y. Bliokh, Geometrodynamics of polarized light: Berry phase and spin Hall effect in a gradient-index medium, J. Opt. A **11**, 094009 (2009).